



Purification of hemicellulose from sugarcane bagasse alkaline hydrolysate using an aromatic-selective adsorption resin



Xin You^{a,b}, Xiao Wang^a, Chen Liang^{a,b,*}, Xinliang Liu^{a,b}, Shuangfei Wang^{a,b}

^a School of Light Industrial and Food Engineering, Guangxi University, Nanning, 530004, China

^b Guangxi Key Laboratory of Clean Pulp & Papermaking and Pollution Control, Nanning, 530004, China

ARTICLE INFO

Keywords:

Hemicellulose
Aromatic-selective adsorption resin
Lignin-carbohydrate complexes
Sugarcane bagasse
Alkaline extraction

ABSTRACT

Alkaline extraction of hemicellulose from lignocellulosic materials is an efficient separation method but also extracts polysaccharides with high proportions of lignin. In this study, aromatic-selective adsorption resin was used to remove lignin in the purification of alkaline-extracted hemicellulose from sugarcane bagasse. The content of lignin in the alkaline extracted hemicellulose decreased and the removal rate reached 89.2% at 1/10 wt ratio of lignin to resin. Resin treatment led to a slight loss of hemicellulose but had a minute effect on its molecular weight and structure. The 2D heteronuclear single quantum coherence (HSQC) NMR analysis of adsorbates suggested that the decrease in carbohydrate contents in the extract resulted from the removal of the lignin-carbohydrate complexes (LCCs) during the resin treatment. It was concluded that the resin treatment had a minute effect on the properties of hemicellulose and could significantly improve its separation and purification.

1. Introduction

Due to limited fuel supply, increasing attention to greenhouse gas emissions and the declining in the competitiveness of the traditional pulp and paper industry and paper mills, has led to the conversion of traditional bleached kraft pulp mills into integrated forest biorefineries to increase revenue (Aldajani & Tschirner, 2010; Huang, Ramaswamy, Al-Dajani, & Tschirner, 2010; Ragauskas et al., 2006). To remain viable, the pulp and paper industry needs to increase revenue by producing bioenergy and biomaterials in addition to wood, pulp and paper products. (Heiningen, 2006; Huang et al., 2019; Silveira et al., 2015). In line with the integrated biorefineries, pulp mills are considering the pre-extraction of hemicelluloses prior to traditional pulp processing, instead of burning the hemicellulose with black liquor. From an economical point of view, new, high value-added products produced from hemicellulose and lignin, rather than cellulose, should pave way for additional sources of income to improve their viability, profitability and global competitiveness (Aldajani & Tschirner, 2010; Huang, He, Du, Min, & Yong, 2016). After cellulose, hemicellulose is considered as the second most abundant renewable component of lignocellulosic biomass and can be used in value-added industrial applications including hydrogels (Karaaslan, Tshabalala, & Buschlediller, 2010; Liu et al., 2016), thermoplastics (Goksu, Karamanlioglu, Bakir, Yilmaz, & Yilmazer, 2007; Gröndahl, Lisa Eriksson, & Gatenholm, 2004; Prakobna, Kisonen, Xu, &

Berglund, 2015), and drug carriers (Billiet, Vandenhoute, Schelfhout, Van, & Dubruel, 2012; Kuzmenko, Hagg, & Toriz, 2014; Meena, Lehnen, & Saake, 2014). In the traditional pulp and papermaking industry, the hemicellulose in black liquor has almost no recovery and utilization (Heiningen, 2007) because of the difficulties in separation and purification. During the kraft pulping process, the hemicellulose in the plant material undergoes a high-temperature alkaline cooking, and a peeling reaction occurs. The oxidation reaction and the alkaline hydrolysis decrease the degree of polymerization, and the degradation mostly results in the formation of oligosaccharide or monosaccharides (Persson, Ren, Joelsson, & Technol, 2009). However, when the alkalinity is not very high, the solubility of hemicellulose can be increased without decreasing its molecular weight. For a cost-effective bioscouring in future, high molecular weight hemicellulose will be essential for applications with high economic values (Cheng, Zhan, Li, & Fu, 2011). Moreover, the separation and purification methods are also the key factors in improving the properties and quality of hemicellulose products. Therefore, development of strategies for improving the separation and purification methods of hemicellulose is extremely valuable.

Plant cell walls contain three major polymers: cellulose, hemicellulose and lignin (Balakshin, Capanema, & Berlin, 2014; Huang et al., 2015). Hemicelluloses usually act as a glue holding cellulose and lignin together, while lignin and polysaccharides (mainly

* Corresponding author at: School of Light Industrial and Food Engineering, Guangxi University, Nanning, 530004, China.

E-mail address: liangchen@gxu.edu.cn (C. Liang).

<https://doi.org/10.1016/j.carbpol.2019.115216>

Received 30 April 2019; Received in revised form 15 August 2019; Accepted 19 August 2019

Available online 19 August 2019

0144-8617/ © 2019 Elsevier Ltd. All rights reserved.

hemicelluloses) are linked by covalent bonds, forming lignin-carbohydrate complexes (LCCs) in plants. There are three main types of LCC linkages: phenyl glycoside (PhGlc), benzyl ethers (BE), and γ -esters (Balakshin, Capanema, Gracz, Chang, & Jameel, 2011; Koshijima & Watanabe, 2003; Zhao et al., 2018). Due to the complexity of the LCC structure in the plant cell wall, it is difficult to separate hemicellulose and lignin completely. Various methods have been used previously for the separation of hemicellulose from plant cell walls (Peng et al., 2011; Sun, Sun, Sun, & Su, 2004; Sun, Cao, Li, Xu, & Sun, 2014; Tunc & Heiningen, 2011). However, high-purity hemicellulose that is completely free of other components has been rarely obtained. In addition, these separation and purification methods lead to varying degrees of degradation in hemicellulose, which is one of the important factors restricting the high value utilization of hemicellulose (Jeong, Um, Kim, & Oh, 2010; Tunc & Heiningen, 2011). Alkaline extraction of hemicellulose from lignocellulosic feedstock is an efficient separation method but also yields polysaccharides with high proportions of lignin (Krawczyk, Oinonen, & Jönsson, 2013; Roos, Persson, Krawczyk, Zacchi, & Ståhlbrand, 2009). Lignin is prone to affinity reaction and dissociates into small molecules in the alkaline, rendering the subsequent separation and purification of hemicellulose more difficult. At present, the most commonly used method for purification of hemicellulose is ethanol precipitation, which is based on the difference in the solubilities of hemicellulose and lignin in organic solvents. However, owing to the presence of LCCs, some lignin still separates out from the extract and remains in the obtained hemicellulose product during precipitation.

An adsorbent with selective adsorption could be a good choice for removing the residual lignin from hemicellulose. Amberlite XAD resins can semi selectively adsorb soluble lignin. The semi selectivity is dependent on the chemical composition of the adsorbent, which is a novel formulation of a styrene-divinylbenzene copolymer that is capable of adsorbing aqueous-soluble hydrophobic molecules through π - π and Van der Waal interactions. Recently, Amberlite XAD resins have been used in biorefineries to obtain lignin from various hydrolysates. For example, Westerberg et al. (2012) has refined the oligosaccharides and lignosulfonates from the hydrolysate of sweet mash using Amberlite XAD 16 N resin. Westerberg et al. (2012) reported that the adsorption of lignin from biomass hydrolysate by XAD resin provided strong evidence of covalently linked carbohydrate segments (LCC structures). However, the explicit proof of LCC connectivity could not be confirmed because of the lack of spectroscopic analysis. Robert H. Narron et al. used nuclear magnetic resonance (NMR) spectroscopy to quantitatively analyze the structure of the adsorbate from the water-pretreated hydrolysate of bagasse (Narron, Chang, Jameel, & Park, 2017). The lignin-carbohydrate complex structure could be identified in the adsorbate, confirming that the carbohydrates adsorbed by XAD were the LCCs. Owing to the selective adsorption of lignin by the XAD resin, it was increasingly used by researcher to purify hemicellulose. For example, Koivula et al. (2013) used Amberlite XAD-7 and XAD-16 resins to treat pre-hydrolysates from birch and pine and found that both the resins could selectively adsorb lignin, thereby providing pure hemicellulose. Despite this, the hemicellulose content was significantly low when higher dosage of the resin was used, although the specific effect of XAD resin on the purification of hemicellulose was not reported.

In this study, the concrete influence of an aromatic-selective adsorption resin on hemicellulose was explored. Amberlite XAD 16 N resin was used to adsorb lignin in hemicellulose from bagasse alkali-extracted bagasse. The lignin removal rate was calculated, and the properties and structure of hemicellulose were analyzed by ion chromatography (IC), 2D heteronuclear single quantum coherence (HSQC) spectroscopy, and gel permeation chromatography (GPC).

2. Materials and methods

2.1. Materials

Sugarcane bagasse was kindly provided by a sugar manufacturer located in Guangxi province, China. Amberlite XAD 16 N resin was purchased from Sigma. Chromatographically pure standard compounds (mannose, glucose, galactose, xylose, and arabinose) were obtained from Sigma. Other chemicals were of analytical grade and used without further purification.

2.2. Alkaline hemicellulose extraction

Alkaline pretreatment was performed in an electrothermal reactor (VRD-42SD-A, CNPPRI, China). Briefly, 1000 g of sugarcane bagasse and 80 g of NaOH were added into the reactor, followed by the addition of 8 L water. Pretreatment temperature was set at 90 °C and maintained for 120 min. After the reaction, the resulting mixture was filtered, and the extract was collected. The pH of the extract was adjusted between 5.5 and 6.0 using 6 M HCl. The resulting suspension was centrifuged, and the supernatant was collected.

2.3. Adsorption on resin

Amberlite XAD 16 N resin was used for lignin adsorption from the alkaline extract. The resin was pretreated using the protocol given by Narron et al. (2017). Before the resin adsorption experiments, the moisture content of the resin was examined. Varying dosages of the resin were added into the alkaline extract according to the weight ratio (g/g) of lignin (lignin content in the extract) to resin (1/1, 1/2, 1/3, 1/5, 1/6, 1/8, 1/10). The mixture was shaken at 150 rpm for 1 h at 30 °C in a constant temperature bath oscillator. The filtrate and resin were collected after filtration; the samples were labeled as x-1, x-2, x-3, x-5, x-6, x-8 and x-10, based on the resin content.

2.4. Desorption from resin

The adsorbate bearing resin was washed with deionized water to remove the unadsorbed alkaline extract. Next, methanol was added to desorb the adsorbed molecules. For each adsorption, the volume of methanol required for desorption was three times that of the starting alkaline extract. The mixture was shaken at 150 rpm for 24 h at 30 °C in the constant temperature bath oscillator. The analyzed resin was separated by filtration, and the methanol filtrate was collected. Next, methanol was evaporated using a rotary evaporator. The obtained solids were resuspended into deionized water and freeze-dried to produce handleable solid adsorbates; the sample were labeled as x-1 J, x-2 J, x-3 J, x-4 J, x-5 J, x-6 J, x-8 J and x-10 J.

2.5. Measurement of lignin content

The lignin content was determined from the absorption at 205 nm, using a UV spectrometer (Agilent 8453, USA) (Miyamoto et al., 2018). The lignin standard was obtained from the alkaline extraction using 1 g XAD-16 resin that was shaken at 150 rpm for 60 min at 30 °C. Desorption was carried out with 3 volumes of methanol, and the adsorbed solid was collected by rotary evaporation as a lignin standard with purity of 98.5%. The lignin content was determined using the following formula:

$$C_i = (n \times A_i) / 89.222$$

Here, C_i is concentration of lignin in g/L, n is dilution ratio, A_i is UV absorbance. All the absorbance values reported here are an average of two measurements. The value of 89.222 was calculated according to the standard curve.

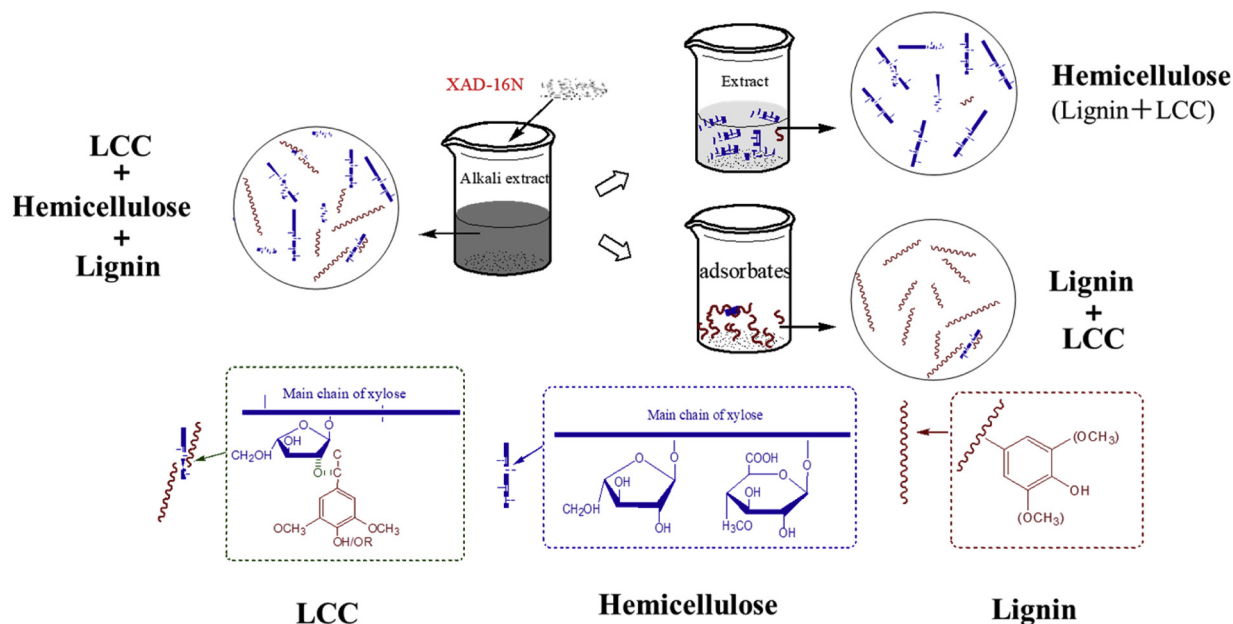


Fig. 1. Schematics of carbohydrate and lignin separation by Amberlite XAD 16 N resin.

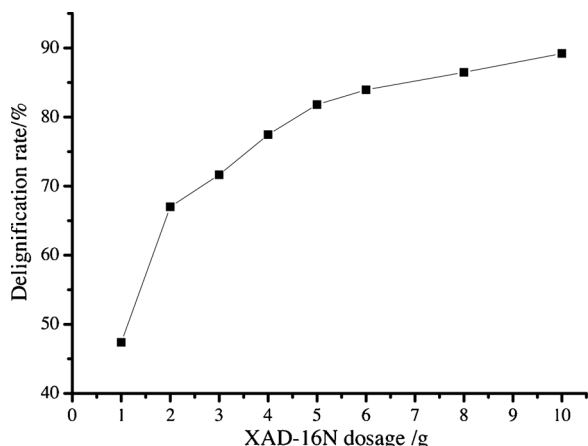


Fig. 2. Isotherms of the delignification rate in the extract plotted against resin dosage.

2.6. Measurement of hemicellulose content

Ion chromatography (ICS-5000+, THERMO, USA) was used to determine the monosaccharide and hemicellulose contents before and after resin adsorption. The standard protocol of the measurement was based on the method given by the National Renewable Energy Laboratory (Sluiter et al., 2008). Calibration was performed with chromatographically pure of glucose, xylose, galactose, mannose, and arabinose. All the values represent an average of two measurements, and the average standard deviation was 1.5%.

2.7. 2D HSQC NMR

The extracts before and after resin treatment were examined. Six volumes of ethanol were used to precipitate the corresponding hemicellulose. After allowing the samples to stand for 10 min, the precipitates were collected by centrifugation. The obtained solids were freeze-dried to produce handleable solid hemicellulose.

All the 2D-HSQC spectra were acquired at 25 °C on a Bruker 500 MHz spectrometer using DMSO-d₆ and D₂O-d₆ as solvents (Huang et al., 2015). The adsorbate concentration was 20% (w/v) (Fig. 1).

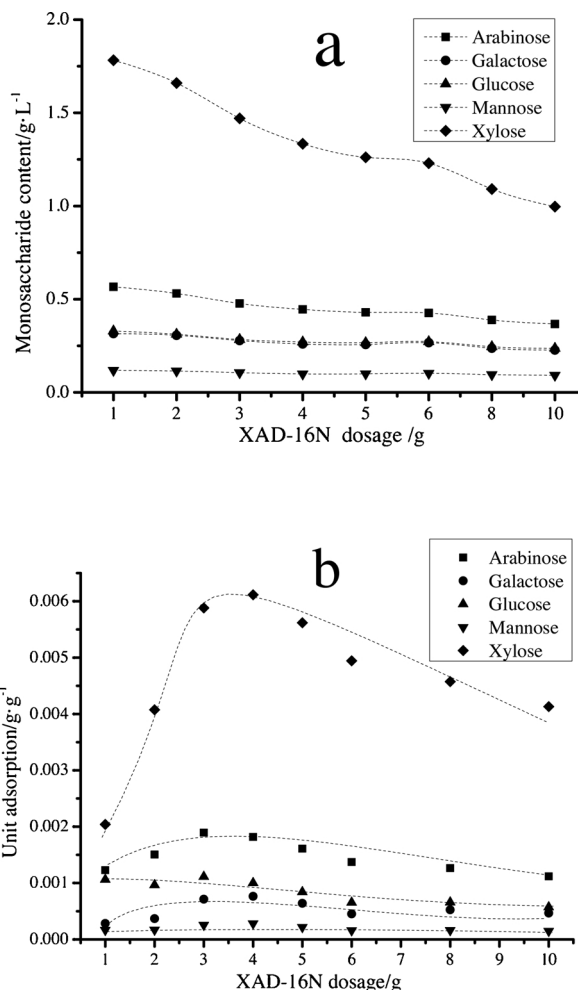


Fig. 3. a) The monosaccharide content in the extract with resin dosage b) The adsorption capacity of static unit volume of resins changes with resin dosage.

Table 1
Molecular weight of alcoholic hemicellulose.

Sample	Mw	Mn	Mw/Mn
Before resin adsorption	7.7×10^4	6.17×10^4	1.25
After resin adsorption(x-3)	6×10^4	4.57×10^4	1.31

2.8. Gel permeation chromatography

The weight-average (*Mw*) and number-average (*Mn*) molecular weights of hemicellulose were estimated by GPC, based on a previous report (Zhao et al., 2016).

3. Results and discussion

3.1. Effect of resin treatment on the rate of delignification

Amberlite XAD resins is an aromatic-selective adsorption resin that can selectively adsorb lignin by π - π and Van der Waals interactions (Sainio, Turku, & Heinonen, 2011) Fig. 2 shows that the delignification rate of the extract increases significantly with increasing resin dosage. When the dosage of the resin is 10 g (lignin/resin = 1/10), the delignification rate of the extract is 89.2%. This indicates that a high dose of resin result in higher adsorption of lignin. However, the lignin removal rate decreases when the resin dosage is increased beyond a certain point. This is because the lignin content in the extract is relatively high, and thus, when the resin dosage is small, the adsorption on the resin is quickly saturated. With increasing resin dosage, more lignin is adsorbed, and the delignification rate is significantly increased. After the resin dosage reaches a certain level, the amount of lignin that is easily adsorbed is reduced. Even though the adsorption on the resin does not reach saturation, the remaining lignin content cannot be adsorbed, thereby resulting in a slower increase in the lignin removal rate. Narron et al. found that a small amount of lignin in the hot water extract of bagasse cannot be adsorbed by XAD resin, due to the weak interaction between lignin and the resin (Narron et al., 2017).

3.2. Effect of resin treatment on hemicellulose

Ion chromatography was used to determine the monosaccharides and hemicellulose content. After resin adsorption, the hemicellulose

content was slightly decreased (Fig. 3a). With the increase in resin dosage, monosaccharide content in the extract is reduced, indicating that a small amount of hemicellulose, along with the benzene ring structure, is adsorbed into the resin. Amberlite XAD resins can selectively adsorb compounds containing benzene ring structures. However, monomeric carbohydrates do not bear the molecular properties suitable for adsorption onto XAD resin. Hence, the adsorbed hemicellulose in the XAD resin should originate from the LCCs. When the dosage of the resin exceeds 10 g, the rate of loss of hemicellulose in the extract is more than 20%. Although a higher resin dosage can remove lignin more effectively, the loss in hemicellulose will also increase. Therefore, the resin dosage should be optimized according to the requirements, to avoid unnecessary loss and reduce the cost.

The adsorption capacity change of static unit volume of resins with resin dosage is shown in Fig. 3b. It can be seen that a small amount of xylose adsorbed by the unit resin when a low dosage of the resin is used, indicating that the xylose unit is not preferentially absorbed by the resin. The main chain of bagasse hemicellulose is formed by linking xylose units. It is speculated that lignin and hemicellulose of the adsorbed LCC structure are not connected to the main chain of hemicellulose. Therefore, small molecule hemicellulose with shorter main chain along with the LCC structure may be adsorbed easily by the resin. After increasing the dosage of the resin, both the amount of xylose adsorbed by the unit resin and the proportion of xylose units in the adsorbed hemicellulose are increased significantly (Fig.3a), which indicates that the length of the xylose main chain of the adsorbed hemicellulose increases as the resin dosage increases. Furthermore, the adsorption capacity of unit volume of resins for the monosaccharide decreases when the resin dosage exceeds 4 g. This is owing to that the less and less residual lignin in the extract caused an unreachable saturated state of the adsorption of resin.

The molecular weight of hemicellulose was determined by GPC (Table 1). The molecular weight (MW) of hemicellulose before and after the resin treatment was 77,000 and 60,000 g / mol, indicating a small change in the molecular weight of the hemicellulose before and after resin treatment. The analyses of monosaccharides and hemicellulose contents indicates that a small amount of hemicellulose with the LCC structure is adsorbed by the resin, resulting in a small change in its molecular weight during the resin treatment.

The effect of resin treatment on hemicellulose structures was analyzed by 2D HSQC analysis of the hemicellulose structure. All the structurally-representative signals and their corresponding chemical

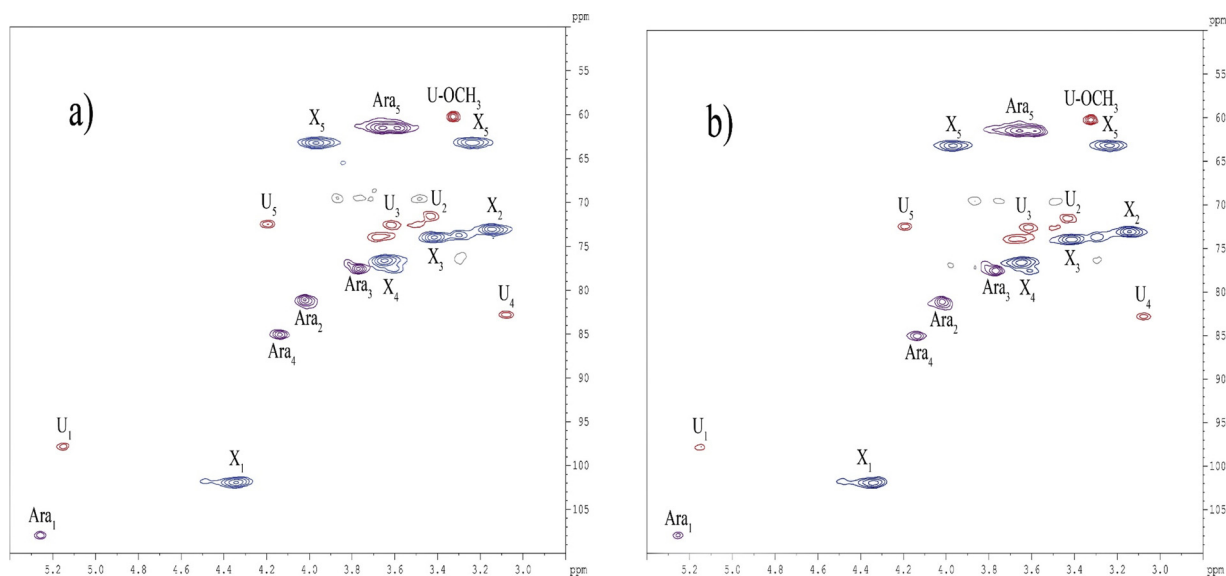


Fig. 4. 2D-HSQC NMR spectra of hemicellulose before(a) and after(b) resin adsorption (D2O as solvent); Carbohydrate signals were labeled as follows: U and X are α -D-GlcUA and β -D-xylopyranoside units, respectively; Ara are α -L-arabinofuranosyl units.

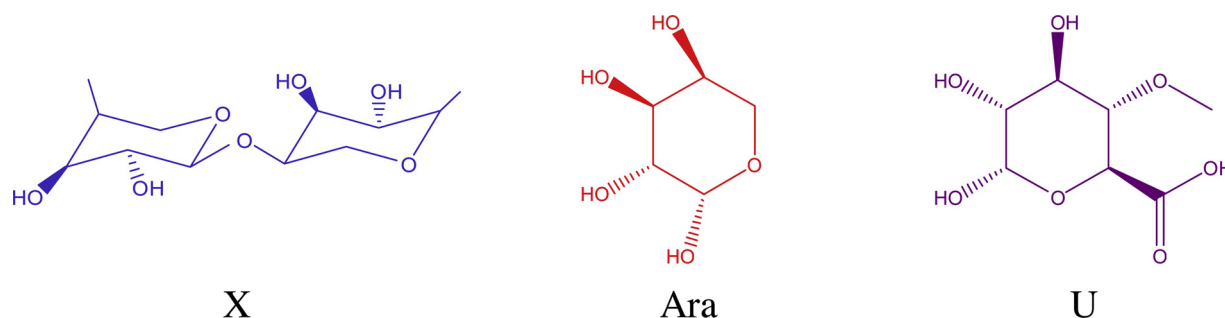


Fig. 5. Hemicellulose main substructure unit(Miyamoto et al., 2018):(X) β -1,4-D-xylopyranoside; (Ara) L-arabinofuranosyl units; (U) 4-O-methyl- α -D-GlcUA.

Table 2
Monosaccharide content in the adsorbate.

	Proportion of monosaccharide components in adsorbate (%)							
	x-1J	x-2J	x-3J	x-4J	x-5J	x-6J	x-8J	x-10J
Arabinose	0.25	0.41	0.46	0.53	0.51	0.56	0.74	0.81
Galactose	0.07	0.11	0.13	0.16	0.16	0.18	0.25	0.30
Glucose	0.42	0.48	0.52	0.56	0.57	0.57	0.66	0.68
Mannose	0.03	0.04	0.03	0.04	0.05	0.04	0.03	0.02
Xylose	0.23	0.37	0.45	0.57	0.55	0.64	0.90	1.05
Total	0.99	1.41	1.59	1.85	1.84	1.99	2.59	2.87

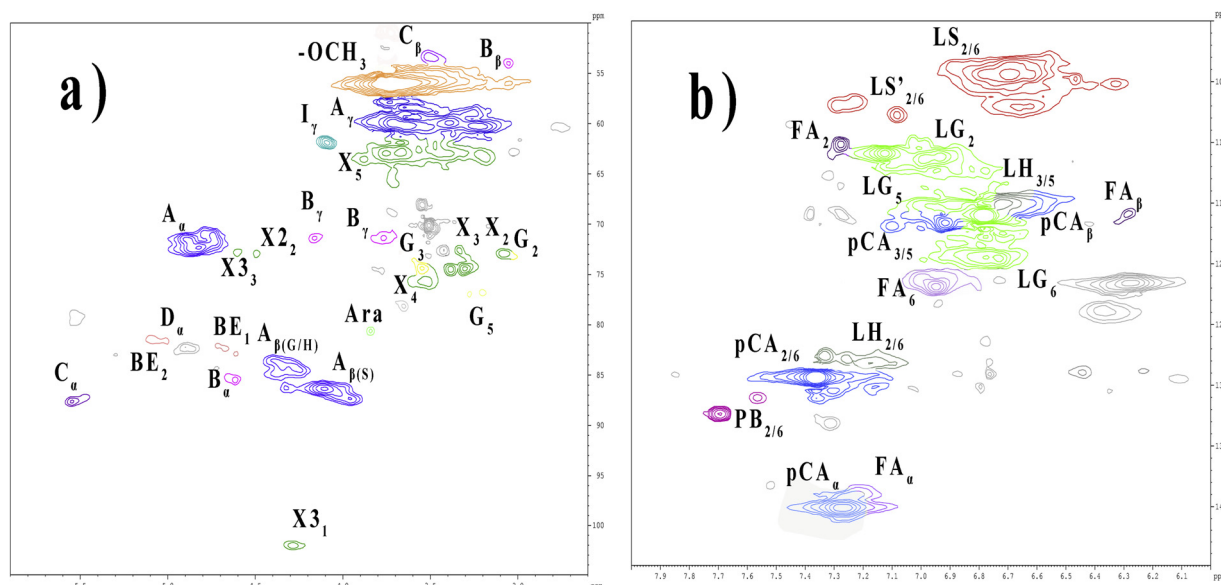


Fig. 6. Side-chain ($\delta C/\delta H$ 50–110/2.5–6.0; a) and aromatic regions ($\delta C/\delta H$ 100–150/6.0–8.0; b) in the 2D HSQC NMR spectra of resin adsorbates. (DMSO- d_6 as solvent).

shifts in 2D-HSQC were identified based on the reputed publications (Mansfield, Kim, Lu, & Ralph, 2012; Miyamoto et al., 2018; Peng et al., 2011; Zhao et al., 2018). The 2D-HSQC signal assignments are shown in the Supporting Information(S1). Various signals from the associated carbohydrates were found in the 2D HSQC spectra of hemicellulose (Fig. 4). The main substructures of hemicellulose are depicted in Fig. 5.

The C–H signal shift of hemicellulose in the spectrum was corrected using the C1–H1 correlation signal peak shift of the xylose unit ($\delta C/\delta H$ 101.9/4.34 ppm). The most important carbohydrates signals observed in hemicellulose before and after purification corresponded to C2–H2 ($\delta C/\delta H$ 72.9/3.14), C3–H3($\delta C/\delta H$ 63.2/3.23), C4–H4($\delta C/\delta H$ 76.5/3.65), and C5–H5($\delta C/\delta H$ 63.3/3.23 and3.97) correlations in xyloans (X2, X3, X4, and X5). In addition, correlations from 4-O-methyl- α -D-GlcUA and α -L-arabinofuranosyl units were observed. In short, the main structural units of hemicellulose before and after the resin

purification were β -1,4 linked D-xylan units (X).There was a negligible signal change in the hemicellulose samples before and after the resin purification. Thus, it can be concluded that the hemicellulose structure is hardly affected during the purification of the resin.

3.3. Composition and structure analysis of resin adsorbates

The ratio of hemicellulose in the total adsorbate of the resin is listed in Table 2. It can be seen that the proportion of hemicellulose in the adsorbate is less than 3%, and the main component of the adsorbate is lignin. The hemicellulose content in the adsorbate increases with resin dosage, and particularly, the xylose unit content increases significantly. This is consistent with the change in hemicellulose content in the extract.

Two-dimensional HSQC spectroscopy can provide important

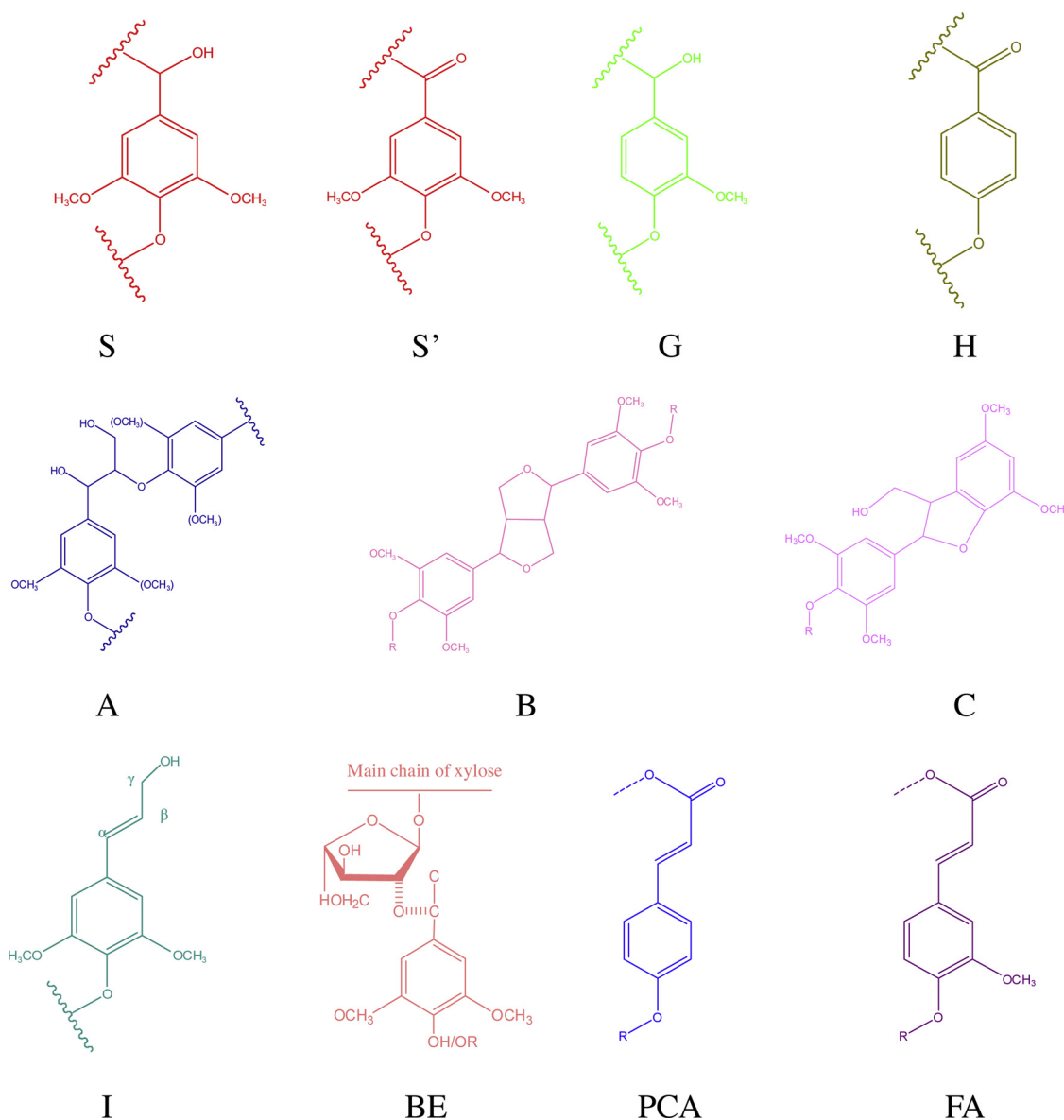


Fig. 7. LCC and lignin main substructure unit (Narron et al., 2017; Stevanic et al., 2014; Zhao et al., 2018): (S) syringyl units; and (S') oxidized syringyl units; (G) guaiacyl units; (H) p-hydroxyphenyl units; (A) β -O-4 linkages; (B) resinol substructures; (C) phenylcoumaran substructures; (I) p-hydroxycinnamyl alcohol end groups; (BE) benzyl ether; (PCA) p-coumarate residues; (FA) ferulate residues.

information on the composition and structure of the LCCs and lignin (Du et al., 2014; Stevanic et al., 2014). In order to determine the LCC structure and the type of linkage in the resin adsorbate, NMR spectra were recorded. All the structurally-representative signals and their corresponding chemical shifts in 2D-HSQC were identified based on previous studies (Balakshin et al., 2011; Del et al., 2012; Du, Gellerstedt, & Li, 2013; Mansfield et al., 2012; Narron et al., 2017; Yuan, Sun, Xu, & Sun, 2011). Two dimensional HSQC signal assignments are displayed in the Supporting Information (S2).

The 2D HSQC spectra (Fig. 6) showed prominent signals ($\delta\text{C}/\delta\text{H}$ 50–90/2.5–6.0), corresponding to methoxy groups and β -O-4 aryl ether linkages for the side-chain regions. Apart from the $\text{C}\alpha$ - $\text{H}\alpha$ and $\text{C}\gamma$ - $\text{H}\gamma$ signals correlations in β -O-4 substructures (A), other substructures were also identified in the spectra of the adsorbates, such as β - β (resinol, B), β -5 (phenylcoumaran, C), and β -1 (spirodienone, D). In the aromatic regions ($\delta\text{C}/\delta\text{H}$ 100–150/6.0–8.0) of the 2D HSQC spectra of the resin adsorbates, aromatic signals from the major lignin units (LS, LG and LH) as well as pCA and FA residues (pCA and FA) were dominant. This indicates that the adsorbate is mainly composed of lignin units (S, G and

H), confirming the strong adsorption capacity of the macroporous resin toward lignin.

In addition to several native lignin structures, signals from visible resonance of LCC in 2D HSQC NMR spectra (Fig. 6, a) suggests the indeed presence of LCC structures in adsorbates. It is generally accepted that there are three main types of LCC linkages: phenyl glycoside (PhGlc) linkage, benzyl ethers (BE) linkage, and γ -ester linkage. The γ -ester linkages were easily dissociated under mild alkaline conditions (Zhao et al., 2018). Hence, no signals from the γ -ester linkages of the obtained LCC at $\delta\text{C}/\delta\text{H}$ 65–62/4.0–4.5 (Balakshin et al., 2011) were observed. There are two types of native benzyl ether LCC linkages (Westerberg et al., 2012): (1) benzyl ethers connecting $\text{C}\alpha$ of lignin to primary hydroxyl groups of carbohydrate and (2) benzyl ethers connecting the $\text{C}\alpha$ of lignin to secondary hydroxyl groups of carbohydrate. However, the signal of BE_2 overlaps with the correlations of $\text{C}\alpha$ - $\text{H}\alpha$ in the spirodienone structure (D) at $\delta\text{C}/\delta\text{H}$ 81.3/5.07 (Balakshin et al., 2011). Hence, we focused on the analysis of BE_1 linkages. The BE_1 ($\delta\text{C}/\delta\text{H}$ 82.0/4.65) signal (Fig. 5(a)), results from the stability of the benzyl ethers linkages under alkaline conditions. Furthermore, signals from

phenyl glycoside (PhGlc) were not observed, indicating that phenyl glycoside (PhGlc) structures are not present in the adsorbates. This further confirms that the LCC structure in the adsorbate is mainly composed of benzyl ethers linkages. This provides reasonable explanation for the carbohydrate of adsorbates.

In the side-chain regions of the adsorbate, the signals of the polysaccharide mainly corresponded to dextran (G), arabinose (Ara), xylan and acetylated xylan (X). This confirmed that the adsorbate contained hemicellulose structure. The signals in this region overlap with each other and overlap with the side chain signal of lignin. Assignments in this region are still in progress, but due to the limitations of the 2D NMR method and its resolution, these overlapped signals mentioned above cannot be fully integrated (Fig. 7).

4. Conclusions

To reduce the of lignin content in the alkali-extracted hemicellulose from bagasse, purification was carried out using aromatic-selective adsorption resin. The lignin content in the alkaline extracted hemicellulose decreased after XAD resin adsorption. The lignin removal rate reach 89.2% at 1/10 wt ratio of lignin to resin. Resin adsorption causes a slight loss of hemicellulose but affects the molecular weight, branching and structure of hemicellulose only slightly. The 2D HSQC NMR analysis of adsorbates suggested that the loss in carbohydrate contents in the extract resulted from the removal of the LCCs during the resin treatment. These results indicated that resin purification can improve the purity of hemicellulose without affecting the other properties. Thus, this strategy can significantly improve the separation and purification process of hemicellulose.

Acknowledgments

This project was supported by the Guangxi Natural Science Foundation of China (2017GXNSFAA198220) and the Guangxi Special Funds for Academic and Technical Leaders.

Appendix A. Supplementary data

Supplementary material related to this article can be found, in the online version, at doi:<https://doi.org/10.1016/j.carbpol.2019.115216>.

References

Aldajani, W. W., & Tschirner, U. W. (2010). Pre-extraction of hemicelluloses and subsequent ASA and ASAM pulping: Comparison of autohydrolysis and alkaline extraction. *Holzforchung*, *64*(4), 411–416.

Balakshin, M., Capanema, E., & Berlin, A. (2014). Chapter 4—isolation and analysis of lignin-carbohydrate complexes preparations with traditional and advanced methods: a review. *Studies in Natural Products Chemistry*, *42*(4), 83–115.

Balakshin, M., Capanema, E., Gracz, H., Chang, H. M., & Jameel, H. (2011). Quantification of lignin-carbohydrate linkages with high-resolution NMR spectroscopy. *Planta*, *233*(6), 1097–1110.

Billiet, T., Vandenhaute, M., Schelfhout, J., Van, V. S., & Dubruel, P. (2012). A review of trends and limitations in hydrogel-rapid prototyping for tissue engineering. *Biomaterials*, *33*(26), 6020–6041.

Cheng, H. L., Zhan, H. Y., Li, B. Y., & Fu, H. Y. (2011). Isolation and characterization of corn stover hemicellulose. *Transactions of China Pulp and Paper*, *19*(2), 259–287.

Del, R., José, C., Rencoret, J., Prinsen, P., Martínez, Á. T., Ralph, J., ... Gutiérrez, A. (2012). Structural characterization of wheat straw lignin as revealed by analytical pyrolysis, 2D-NMR, and reductive cleavage methods. *Journal of Agricultural and Food Chemistry*, *60*(23), 5922.

Du, X. Y., Gellerstedt, G., & Li, J. B. (2013). Universal fractionation of lignin-carbohydrate complexes (LCCs) from lignocellulosic biomass: An example using spruce wood. *The Plant Journal*, *74*(2), 328–338.

Du, X., Pérez-Boada, M., Fernández, C., Rencoret, J., Del Río, J. C., Jiménez-Barbero, J., ... Martínez, A. T. (2014). Analysis of lignin-carbohydrate and lignin-lignin linkages after hydrolase treatment of xylan-lignin, glucomannan-lignin and glucan-lignin complexes from spruce wood. *Planta*, *239*(5), 1079–1090.

Goksu, E. I., Karamanlioglu, M., Bakir, U., Yilmaz, L., & Yilmazer, U. (2007). Production and characterization of films from cotton stalk xylan. *Journal of Agricultural and Food Chemistry*, *55*(26), 10685–10691.

Gröndahl, M., Lisa Eriksson, A., & Gatenholm, P. (2004). Material properties of plasticized

hardwood xylans for potential application as oxygen barrier films. *Biomacromolecules*, *5*(4), 1528–1535.

Heiningen, A. V. (2007). Converting a kraft pulp mill into an integrated forest biorefinery. *World Pulp & Paper*, *107*(6), 38–43.

Huang, C. X., Chu, Q. L., Xie, Y. H., Li, X., Jin, Y. C., Min, D. Y., ... Yong, Q. (2015). Effect of kraft pulping pretreatment on the chemical composition, enzymatic digestibility, and sugar release of moso bamboo residues. *Bioresources*, *10*(1), 240–255.

Huang, C. X., Dong, H. L., Su, Y., Wu, Y., Narron, R., & Yong, Q. (2019). Synthesis of carbon quantum dot nanoparticles derived from byproducts in bio-refinery process for cell imaging and in vivo bioimaging. *Nanomaterials*, *9*(3).

Huang, C. X., He, J., Du, L. T., Min, D. Y., & Yong, Q. (2016). Structural characterization of the lignins from the green and yellow bamboo of bamboo culm (*Phyllostachys pubescens*). *Journal of Wood Chemistry and Technology*, *36*(3), 157–172.

Huang, H. J., Ramaswamy, S., Al-Dajani, W. W., & Tschirner, U. (2010). Process modeling and analysis of pulp mill-based integrated biorefinery with hemicellulose pre-extraction for ethanol production: A comparative study. *Bioresource Technology*, *101*(2), 624–631.

Jeong, T. S., Um, B. H., Kim, J. S., & Oh, K. K. (2010). Optimizing dilute-acid pretreatment of rapeseed straw for extraction of hemicellulose. *Applied Biochemistry and Biotechnology*, *161*(1–8), 22–33.

Karaaslan, A. M., Tshabalala, M. A., & Buschlediger, G. (2010). Wood hemicellulose/chitosan-based semi-interpenetrating network hydrogels: Mechanical, swelling and controlled drug release properties. *Bioresources*, *5*(2), 1036–1054.

Koivula, E., Kallioinen, M., Sainio, T., Antón, E., Luque, S., & Mänttari, M. (2013). Enhanced membrane filtration of wood hydrolysates for hemicelluloses recovery by pretreatment with polymeric adsorbents. *Bioresource Technology*, *143*(17), 275–281.

Koshijima, T., & Watanabe, T. (2003). *Association between lignin and carbohydrates in wood and other plant tissues*. Berlin Heidelberg: Springer.

Krawczyk, H., Oinonen, P., & Jönsson, A. S. (2013). Combined membrane filtration and enzymatic treatment for recovery of high molecular mass hemicelluloses from chemithermomechanical pulp process water. *Chemical Engineering Journal*, *225*(225), 292–299.

Kuzmenko, V., Hagg, D., & Toriz, G. (2014). In situ forming spruce xylan-based hydrogel for cell immobilization. *Carbohydrate Polymers: Scientific and Technological Aspects of Industrially Important Polysaccharides*, 862–868.

Liu, J., Chinga-Carrasco, G., Cheng, F., Xu, W., Willför, S., Syverud, K., ... Xu, C. (2016). Hemicellulose-reinforced nanocellulose hydrogels for wound healing application. *Cellulose*, *23*(5), 1–15.

Mansfield, S. D., Kim, H., Lu, F., & Ralph, J. (2012). Whole plant cell wall characterization using solution-state 2D NMR. *Nature Protocols*, *7*(9), 1579–1589.

Meena, R., Lehnen, R., & Saake, B. (2014). Microwave-assisted synthesis of kC/Xylan/PVP-based blend hydrogel materials: Physicochemical and rheological studies. *Cellulose*, *1*, 553–568.

Miyamoto, T., Mihashi, A., Yamamura, M., Tobimatsu, Y., Suzuki, S., Kojima, M., ... Umezawwa, T. (2018). Comparative analysis of lignin chemical structures of sugarcane bagasse pretreated by alkaline, hydrothermal, and dilute sulfuric acid methods. *Industrial Crops and Products*, 121.

Narron, R. H., Chang, H. M., Jameel, H., & Park, S. (2017). Soluble lignin recovered from biorefinery pretreatment hydrolyzate characterized by lignin-carbohydrate complexes. *ACS Sustainable Chemistry & Engineering*, *5*(11).

Peng, P., Peng, F., Bian, J., Xu, F., Sun, R. C., & Kennedy, J. F. (2011). Isolation and structural characterization of hemicelluloses from the bamboo species *Phyllostachys incarnata* Wen. *Carbohydrate Polymers*, *86*(22), 883–890.

Persson, T., Ren, J. L., Joëlsson, E., & Technol, A.-S. J. J. B. (2009). Fractionation of wheat and barley straw to access high-molecular-mass hemicelluloses prior to ethanol production. *Bioresource Technology*, *100*(17), 3906–3913.

Prakobna, K., Kisonen, V., Xu, C., & Berglund, L. A. (2015). Strong reinforcing effects from galactoglucomannan hemicellulose on mechanical behavior of wet cellulose nanofiber gels. *Journal of Materials Science*, *50*(22), 7413–7423.

Ragauskas, A. J., Nagy, M., Kim, D. H., Eckert, C. A., Hallett, J. P., & Liotta, C. L. J. B. (2006). *From wood to fuels: Integrating biofuels and pulp production*. *2*(1), 55–56.

Roos, A. A., Persson, T., Krawczyk, H., Zacchi, G., & Ståhlbrand, H. (2009). Extraction of water-soluble hemicelluloses from barley husks. *Bioresource Technology*, *100*(2), 763–769.

Sainio, T., Turku, I., & Heinonen, J. (2011). Adsorptive removal of fermentation inhibitors from concentrated acid hydrolyzates of lignocellulosic biomass. *Bioresource Technology*, *102*(10), 6048–6057.

Silveira, M. H. L., Morais, A. R. C., Costa Lopes, A. M. D., Oleksyszyn, D. N., Bogel-Lukasik, R., Andreas, J., ... Pereira Ramos, L. (2015). Current pretreatment technologies for the development of cellulosic ethanol and biorefineries. *Chemsuschem*, *8*(20), 3366–3390.

Sluiter, A., Hames, B., Ruiz, R., Scarlata, C., Sluiter, J., Templeton, D., ... Crocker, D. J. L. (2008). Determination of structural carbohydrates and lignin in biomass. *Laboratory analytical procedure*, 1617, 1–16.

Stevanic, J. S., Mikkonen, K. S., Xu, C., Tenkanen, M., Berglund, L., & Salmén, L. (2014). Wood cell wall mimicking for composite films of spruce nanofibrillated cellulose with spruce galactoglucomannan and arabinoglucuronoxylan. *Journal of Materials Science*, *49*(14), 5043–5055.

Sun, J. X., Sun, X. F., Sun, R. C., & Su, Y. Q. (2004). Fractional extraction and structural characterization of sugarcane bagasse hemicelluloses. *Carbohydrate Polymers*, *56*(2), 195–204.

Sun, S. N., Cao, X. F., Li, H. Y., Xu, F., & Sun, R. C. (2014). Structural characterization of residual hemicelluloses from hydrothermal pretreated Eucalyptus fiber. *International Journal of Biological Macromolecules*, *69*(8), 158–164.

Tunc, M. S., & Heiningen, A. R. P. V. (2011). Characterization and molecular weight distribution of carbohydrates isolated from the autohydrolysis extract of mixed

- southern hardwoods. *Carbohydrate Polymers*, 83(1), 8–13.
- Westerberg, N., Sunner, H., Helander, M., Henriksson, G., Lawoko, M., & Rasmuson, A. (2012). Separation of galactoglucomannans, lignin, and lignin-carbohydrate complexes from hot-water-extracted norway spruce by cross-flow filtration and adsorption chromatography. *Bioresources*, 7(4), 4501–4516.
- Yuan, T. Q., Sun, S. N., Xu, F., & Sun, R. C. (2011). Characterization of lignin structures and lignin–Carbohydrate complex (LCC) linkages by quantitative ¹³C and 2D HSQC NMR spectroscopy. *Journal of Agricultural and Food Chemistry*, 59(19), 10604–10614.
- Zhao, B. C., Chen, B. Y., Yang, S., Yuan, T. Q., Charlton, A., & Sun, R. C. (2016). Structural variation of lignin and lignin-carbohydrate complex in *Eucalyptus grandis* × *E. urophylla* during its growth process. *ACS Sustainable Chemistry & Engineering*, 5(1).
- Zhao, B. C., Xu, J. D., Chen, B. Y., Cao, X. F., Yuan, T. Q., Wang, S. F., ... Sun, R. C. (2018). Selective precipitation and characterization of lignin-carbohydrate complexes (LCCs) from *Eucalyptus*. *Planta*, 247(5), 1–11.